Kinetics of release and antibacterial activity of salicylic acid loaded into halloysite nanotubes

L. Ghezzi[a], A. Spepi, M. Agnolucci[b], C. Cristani[b], M. Giovannetti[b], M.R Tinè[a], C. Duce[a,*]

[a]Department of Chemistry and Industrial Chemistry, University of Pisa, Via Moruzzi 3, I-56124 Pisa, Italy.

[b]Department of Agriculture, Food and Environment, University of Pisa, Via del Borghetto 80, I-56124 Pisa, Italy

Corresponding author: celia.duce@unipi.it

Abstract

In this work halloysite (Hal) nanotubes were used as nanocontainers for salycilic acid (SA) in a perpective of its use in active packaging for food industry. The system Hal/SA was investigated for its ability to stabilize Hal suspensions by turbidimetry, its release kinetics in water by UV spectroscopy and its antibacterial activity against *Pseudomonas fluorescens* IMA 19/5 by Isothermal Micro Calorimetry (IMC). IMC is a sensitive and non destructive technique and allows the study of a wide range of relatively slow processes (hours and days) in solutions. The system Hal/SA resulted to stabilize Hal suspension in water and to release SA in a controlled way over 50h. Moreover the SA released by Hal/SA showed an antibacterial activity at lower concentrations than free SA, likely due to the close contact of bacteria and Hal in the reaction vessel.

Keywords: Halloysite nanotubes; Salicylic acid; *Pseudomonas fluorescens*; antibacterial activity Isothermal Micro Calorimetry (IMC); Turbidimetry; UV spectroscopy

1. Introduction

Halloysite (Hal) nanotubes are naturally occurring aluminosilicate that have been massively exploited as nanocontainers in recent years due to their biocompatibility and absent cytotoxicity at concentrations up to 0.2 mg/ml (Lai et al., 2013; Lvov et al., 2014; Massaro et al., 2017; Vergaro et al., 2010). In particular, Hal has a hollow tubular structure of 10-15 bilayers of aluminosilicate layers with SiOH and AlOH groups on the external and internal surfaces, respectively (Abdullayev et al. 2012; Massaro et al., 2017, Yuan et al., 2015). The Hal dimensions depends on the Hal deposit, with a length of 0.2-1.5 μm and inner and outer diameters of 10-30 nm and 40-70 nm, respectively (Abdullayev et al. 2012; Massaro et al., 2017, Yuan et al., 2015). Several works investigated the properties of pristine and modified Hal (Bretti et al., 2016; Duce et al., 2015; Massaro et al., 2017; Presti et al., 2016), its loading and sustained release of active chemical and biochemical molecules (Abdullayev and Lvov., 2016; Aguzzi et al., 2013; Della Porta et al., 2016; Duce et al., 2017; Li et al., 2016; Lun et al., 2014; Lvov et al., 2013; Viseras et al., 2008 Tan et al., 2014; Yuan et al., 2012;) and its possible use in composite and materials with tailored properties (Massaro et al., 2017; Lvov et al., 2013; Zhang et al., 2016).

Salicylic acid (SA) is a natural compound used in a wide range of pharmaceutical formulations and as an additive for food (Baxter et al., 2001) and cosmetics (Coleman and Brody, 1997) due to its bactericidal and antiseptic properties. Moreover it is used to model natural organic matter (NOM) in both experimental and theoretical studies of NOM adsorption on different kinds of mineral surfaces, including clays (Biber and Stumm, 1994; Biddeci et al., 2016; Kubicki et al., 1997; Makaremi et al., 2017; Yost et al., 1990).

The system Hal/SA was previously obtained and characterized (Spepi et al., 2016). Different experimental conditions were tried in order to obtain the maximum loading of SA. The better results were obtained using Hal etched with H_2SO_4 2 M at 25 °C for 48 h and a solution of sodium salicylate (NaSA) at pH 8. As reported previously (Abdullayev et al. 2012; Yuan et al., 2015), mild acid or alkaline treatments slightly enlarged the Hal lumen, but substantially maintained Hal structure. Indeed, SEM X-ray elemental analysis showed that Hal pre-treated with H_2SO_4 2 M at 25 °C for 48 h etching slightly reduced the aluminum/silicon ratio from 1, for pristine Hal, to 0.8 for etched Hal, while SEM images revealed that the nanotubes structure was maintained. (Spepi et al., 2016) Nitrogen Adsorption/Desorption Isotherms showed also a similar pore distribution for Hal etched at 25 °C and pristine Hal, with a slightly higher pore volume and BET surface area (BET area (m^2/g): 70.9 pristine Hal; 113.6 etched Hal; Pore volume (mL/g): 0.1637 pristine Hal; 0.2488 etched Hal).

The pH of the NaSA loading solution was set to 8 in order to maximize the negative charge of salicylate, while remaining within the pH range of 4−8.5 where the inner surface of HNTs was

positively charged. (Abdullayev et al., 2012; Spepi et al., 2016; Yuan et al., 2015) Under such conditions, TG and TG-FTIR data showed that the amount of salicylate retained was 10.5% (w/w) and that the NaSA thermal degradation was drastically modified, when NaSA was located inside Hal, suggesting a strong interaction of the salicylate moiety chemisorbed on the aluminum hydroxide surface. Scanning transmission electron microscopy (STEM) revealed that after NaSA loading, the empty lumen of the HNT was no longer visible (Spepi et al., 2016). NaSA inside Hal lumen produced a partial pore blockage and a reduction in the BET area, micropore area, micropore volume parameters, and mesoporosity of the material. ATR−FTIR interfacial spectra revealed that the Ph−OH group seemed to be involved in the interaction between salicylate and aluminum, with a weakening of the hydrogen bond. The splitting of the ν_{as} and ν_{s} of $-COO^{-}$ into two components suggested the presence of different complexes Hal/SA. The experimental spectra seemed to refer to an NaSA molecule in solution and adsorbed in Hal with a large number different configurations and DFT calculations indicated that the salicylate preferred to adsorb in a monodentate and bridging mode rather than a bidentate mode. In fact, the vibrational spectra of the monodentate and bridging adsorbate models also compared better with the experimental one (Spepi et al., 2016).

To the best of our knowledge, data on the behaviour of Hal/SA system in suspension in aqueous medium are lacking, although they could be exploited in a perspective of Hal/SA use in active packaging for food industry. The concept of active food packaging was developed in the last decade and entails not only food protection, but also positive effects on its safety. One of the most interesting example was the incorporation of antimicrobial compounds into food packaging materials (Galotto et al, 2015). When antimicrobial substances are incorporated into polymers, such antimicrobial films release active compounds and display continuous antimicrobial effects on the food surface during the exposure time, thus increasing consumer safety as the antimicrobial compounds are included in the packaging structure (instead of being directly added to food) and are released in small amounts on the food surface. According to literature, the packaging industry already focused its attention on polymer-clay nanocomposites (Azeredo, 2009) and, even if montmorillonite was the most studied clay filler, there is increasing research interest in potential applications of Hal as filler for polymer nanocomposites (Pasbakhsh et al, 2016). To this aim, Hal nanotubes were tested very recently as active food-packaging material based on starch-halloysite nanocomposites incorporating antimicrobial peptides (Meira et al, 2017) and on poly-lactic acid(PLA)-halloysite nanocomposites using Hal as nanocontainers to carry antimimicrobial ZnO agent within the PLA matrix (De Silva et al, 2015).

Concerning future applications, the use of SA loaded Hal in polymer nanocomposites appears very promising. Besides reinforcement of the food packaging materials, the new formed nanostructure

could provide an additional antimicrobial activity thanks to the loaded SA (as already observed by De Silva et al.2015).

Most of nano-additives (including Hal) were incorporated at 0.1-5% w/w in the packaging material, particularly films. They may be incorporated into polymers by melt- or solvent-compounding. Thermal polymer processing methods, such as extrusion and injection molding, may be used with thermally stable antimicrobials. SA doped Hal can withstand temperatures up to 200-300 °C and therefore could be incorporated as a thin co-extruded layer with processable polymers at such temperature range. The polymer could be selected from the group consisting of polyethylene (PE), poly(vinyl alcohol) (PVA) and bio-based plastics and their blends, that are commonly used in food packaging (Galotto et al. 2015). As organic polymers are not soluble in water or polar solvents, the melt compounding is preferred. Conversely, for polymers like PVA or its blends, the nanocomposite can be also prepared in solution, i.e. by ultrasonicating SA-doped HNTs in the polymer solution.

Exfoliated nanocomposites were reported to exhibit the best properties due to the optimal interaction clay/polymer (Azaredo et al, 2009). Exfoliation could be attained via previous chemical modification of the Hal, for example by using organic ammonium ions which help improve the compatibility with organic polymers.

Data on the behaviour of Hal/SA system in suspension are useful to understand the mechanism of Hal aggregation in water and to investigate different ways to stabilize Hal dispersions. In fact, the absorption of negatively charged molecules inside Hal lumen enhanced the Hal dispersion stability by increasing the net negative charge and electrostatic repulsion of Hal (Cavallaro et al., 2012).

The *in vitro* release studies of encapsulated molecules (drugs, proteins, DNA, corrosion inhibitors etc.) showed a controlled release in aqueous medium that can be further extended by exploiting tube-stoppers, shells and the creation of Hal-polymer nanocomposites (Lvov et al., 2013, 2014). The profile of guest molecules release from Hal lumen was widely described and discussed in terms of Peppas model (Lvov et al., 2013). Differently, the group of Viseras proposed a model based on a combination of first order desorption kinetics that successfully fitted the 5-aminosalicylic acid release from Hal (Aguzzi et al., 2013; Viseras et al., 2008).

In vitro antibacterial, antimicrobial and anticancer tests of new Hal formulations are generally performed by monitoring selected bacterial or cellular/microbial activity on Petri plates added with Hal complexes and comparing it with their standard growth (Abdullayev et al., 2009; Biddeci et al., 2016; Lvov et al., 2013; Makaremi et al., 2017; Riela et al., 2014). In this work, the antibacterial activity of pure SA and Hal/SA system was tested against *P. fluorescens* by using Isothermal Micro Calorimetry (IMC) in order to have direct information of Hal/SA antimicrobial activity in aqueous suspension. IMC measures the heat involved in biological processes *in vitro* and it is successfully

employed for microorganism detection and discrimination, studies of microbial processes and tests of antimicrobial and antibacterial activities of various chemicals (Braissant et al., 2010a, b, 2013; Velazquez et al., 2014; Von Ah et al., 2009). IMC is a sensitive and non-destructive technique and allows the study of a wide range of relatively slow processes (hours and days) in solutions. Microbial cultures in liquid media are placed in the measurement vessel and the heat flow signal is registered. The inoculum of the active agent on the microbial cultures modifies or inhibits the heat evolved. IMC is a promising tool for medical, environmental and food microbiology. (Braissant et al., 2010a, b; Gardikis et al., 2017; Rong et al., 2007; Von Ah et al., 2009)

The aim of this work was to characterize the behaviour of Hal/SA in aqueous medium. In particular Hal/SA was here investigated for its capability of stabilizing Hal suspensions by turbidimetry, for its release kinetics in water by UV spectroscopy and for its antibacterial activity against *Pseudomonas fluorescens* IMA 19/5, a bacterial species active in food spoilage (Gram et al., 2002), by Isothermal Micro Calorimetry (IMC).

2. Experimental

2.1 Materials

Pristine halloysite nanotubes, Sodium salycilate (NaSA) (99.5%), NaOH (≥ 97.0, pellets) were purchased from Sigma Aldrich and used without further purification. SA loaded Hal (Hal/SA) was prepared according to the literature (Duce et al., 2017; Spepi et al., 2016). The suspension of Hal in water was prepared by adding 5 g of etched Hal to a concentrated solution of NaSA in water (1 g/ml) and the pH was adjusted at 8 with NaOH 0.1 M. The suspension was evacuated in a vacuum jar, kept under vacuum for 3 h, and then cycled back to atmospheric pressure. This process was repeated three times. Finally, Hal was separated from the solution by centrifugation, washed with water, dried in an oven at 70°C. The amount of salicylate retained was determined by thermogravimetry resulting in a 10.5% (w/w). The characterization of the empty and loaded systems by means of SEM, SEM X-ray Elemental Analysis, STEM, TG, TG-FTIR, Nitrogen Adsorption/Desorption Isotherms was reported in Spepi et al., 2016. *Pseudomonas fluorescens* IMA 19/5 was obtained from the International Microbial Archives of the Microbiology Laboratories of the Department of Agriculture, Food and Environment (DAFE), University of Pisa.

2.2 Apparatus and methods

2.2.1 UV-VIS spectrometry. A Cary 50-probe UV-Visible Spectrophotometer (Varian) equipped with Xenon flash lamp was used to determine the SA concentration in aqueous media during the release experiments and for the turbidity measurements. The molar extinction coefficients of SA (both in the acid, SA, and monoprotonated, SA^-, form) were previously determined by reading the maximum absorbance in the wavelength range from 250 to 350 nm of SA solutions of known concentrations and pH and by taking into account the dissociation constants of SA (Ernst and Menashi, 1962) and the Lambert-Beer law.

ε_{SA} = da 3608 a 3821 media 3714
ε_{SA^-}= da 3512 a 3750 media 3631

2.2.2 Evaluation of SA release kinetics

The SA release kinetics was evaluated in water at pH = 6-7 (where a mixture of acid SA and anionic SA^- form are present) and at room temperature. 10 mg of Hal/SA were added to 26 ml of deionized water and the suspension was constantly stirred. Samples for analysis were separated from the suspension by centrifugation at 4000 rpm for 4 min. SA concentration in the collected supernatant was measured by UV spectrometry by reading the maximum absorbance in the wavelength range from 250 to 350 nm and taking into account that SA under these pH conditions is mainly in the acidic form. The zero time was taken when Hal was added to water.

2.2.3 Turbidity

To determine the kinetics of sedimentation, the Hal was added to water at a concentration of 1 (w/w%) and stirred vigorously for 15 s before starting the experiment. The experiments were performed by UV-VIS spectrometry, by recording the transmittance at 600 nm as a function of time. In all the experiments a quartz cuvette with a 1 cm path length was employed.

2.2.4 Bacterial cultures

Pre-cultures of *P. fluorescens* IMA 19/5 were grown overnight in 15 mL tubes with 4 mL of Tryptic Soy Broth (TSB; Fluka) medium incubated at 28 °C on a rotating shaker at 150 rpm. Before each IMC experiment bacterial cultures were prepared from precultures inoculating 2 mL of TSB to a final concentration of 0.03 OD (600 nm), corresponding to $1.04 \pm 0.1 \times 10^7$ CFU/mL.

2.2.5 IMC experiments

Isothermal Microcalorimetric (IMC) measurements were performed by a Thermal Activity Monitor 2277 (TA Instruments) equipped with a 4 ml sealed glass ampoule at 25°C.

A stock solution of NaSA 1M was prepared. For each experiment with free salycilate, aliquots of the cultures (OD = 0.03) prepared as previously described, were added with an aliquot of an NaSA 1M stock solution in order to obtain 2 ml of final solution with salycilate concentration of 5, 10, 20, and 30 mM. For each experiment with Hal loaded with SA, 2 ml aliquots of the cultures (OD=0.03) were added with an aliquot (from 13.7 to 82.3 mg) of Hal/SA to give a final salycilate concentration of 5, 10, 20 and 30 mM. The heat released by 2 ml cultures in TSB and by 2 ml cultures in TSB added with 82.3 mg of pristine Hal (the maximum of the quantities used in the Hal/SA experiments), was also measured as reference.

3. Results and discussion

The first part of this work deals with the characterization of Hal/SA dispersion in water and of the kinetics of SA release. The second part evaluates the Hal/SA antibacterial activity against *P. fluoresces* IMA 19/5 in comparison with that of NaSA solutions. IMC results obtained by adding different quantities of SA to *P. fluorescens* IMA 19/5 originating from Hal/SA and NaSA solutions are presented and analyzed.

3.1 Stability of Hal/SA dispersion in water and Kinetics of SA release

The evaluation of the stability of Hal dispersions in water is important in the framework of their application as delivery systems in liquid media. To this aim the kinetics of sedimentation of Hal/SA in water was studied by means of turbidimetry and compared with that of pristine Hal, as reported in Figure 1. The turbidity value of Hal/SA dispersions after equilibration (3h) was higher than those of pristine Hal indicating that the presence of SA into Hal lumen stabilized Hal dispersions. According to the literature (Bretti et al., 2016; Cavallaro et al., 2012), this behaviour can be explained on the basis of enhancement of repulsive electrostatic forces between Hal/SA. The net negative charge of Hal results increased by the partial neutralization of their internal positive charge for the effect of the SA loading.

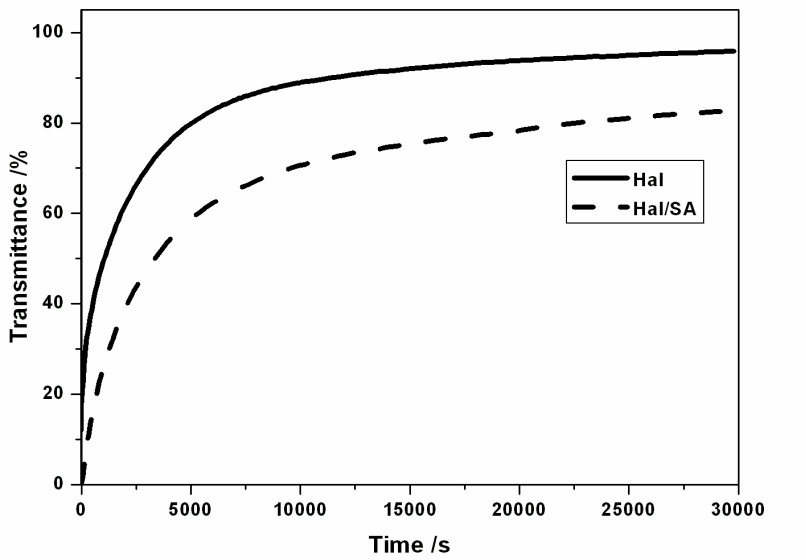

Figure 1: Trasmittance as a function of time for Hal and Hal/SA dispersions (1 w/w%) in water

Release characteristics of Hal/SA are given in Figure 2. The NaSA dissolution in water was very fast and can be considered almost instantaneous, but when NaSA was loaded into Hal lumen, the kinetics of its release took up to 50 h. The 60 % of salycilate was released in the first 10 h and the remaining 40% in the next 40-50 h. This behavior is typical of several molecules loaded into Hal. (Abdullayev, et al., 2009, 2011; Lvov et al., 2013; Wenbo et al., 2014). The fast release of the initial 30% of SA was attributed in literature (Abdullayev et al., 2009) to the dissolution of molecules contained in tube fines and loosely rolled surface clay sheets.

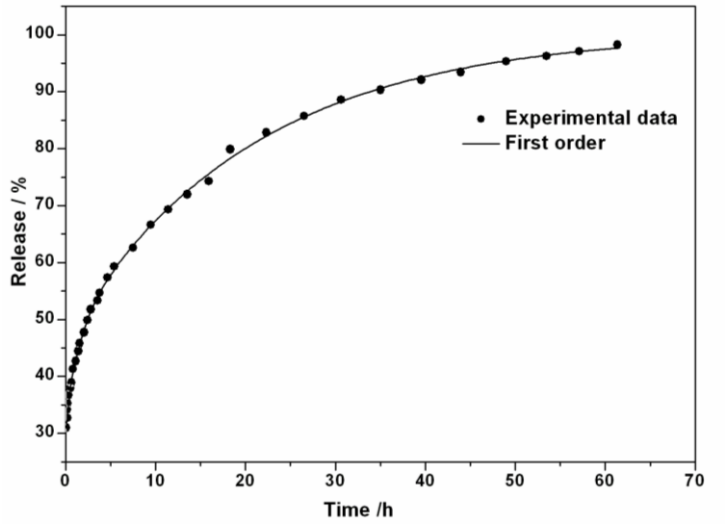

Figure 2: Kinetic release of SA loaded into Hal lumen.

At first, the SA release profile from Hal lumen was fitted following the approach proposed by Viseras group in the paper Aguzzi et al., 2013. The overall release process was seen as a combination of three first order simple desorption processes and the SA release was satisfactory described by the three-exponential reported in Table 1.

In the work Aguzzi et al., 2013, the release curve of 5-aminosalicilic acid (5-ASA) from Hal showed a release of almost 70% within 0.2 h and a complete 5-ASA release within 5 h. This behaviour was satisfactory described by the sum of two first order desorption processes: the very fast desorption of 5-ASA from the external particle surface/and or inter-particle spaces followed by a slower release of small amount of 5-ASA penetrated in tube fines. The loading procedure adopted by the authors, in fact, simply implied the stirring of Hal in a 5-ASA aqueous solution for 24 h and did not included vacuum treatments, thus resulting in a low loading percent (0.4 % w/w). The 5-ASA- Hal adsorbate was then recovered by filtration without washing and dried in oven at 60°C. Under these experimental conditions the majority of 5-ASA probably resulted adsorbed on the Hal surface and in the first part of Hal lumen.

The three cycles of evacuation of the suspension in a vacuum jar and its maintenance under vacuum for 3 h allowed us to obtain a higher and deeper loading. K_1 and K_2 values that we obtained for SA release were similar to those obtained for 5-ASA, thus suggesting that also in our case the SA release started with the desorption from the external particle surface (K_1) followed by the release of SA in tube fines (K_2) and a slower release from the interior of Hal lumen, accounted by K_3.

The equations used, the kinetic constants obtained and the correlation coefficients (R^2) are reported in Table 1.

Table 1: Fitting equations and parameters of the models combining three sequential first order desorption processes

First order[a]						
$ft = C_1 * \left(1 - e^{-K_1 * t/C1}\right) + C_2 * \left(1 - e^{-K_2 * t/C2}\right) + C_3 * \left(1 - e^{-K_3 * t/C3}\right)$						
C1	K_1	*C2*	K_2	*C3*	K_3	R^2
32.2 ± 0.5	1380 ± 187	14.5 ± 0.9	9.8 ± 1.1	53.7 ± 0.7	2.6 ± 0.1	0.9992

[a] ft is the fraction of SA released in time t; C_1, C_2, C_3 are the equilibrium fraction of SA of the three processes; K_1, K_2 and K_3 are the co-first order release constants of the three release processes

The Peppas model (Abdullayev et al., 2009; Aguzzi et al., 2013; Li et al., 2016; Lvov et al., 2013; Peppas, 1985; Tan et al., 2014; Viseras et al., 2008; Wei et al., 2014) was also tested on our data of SA release with comparison purposes. This model, without the original model based on Peppas theory

(Peppas, 1985) can be used rigorously to fit the release data up to 60% of release, but it is also used in literature as empirical equation, known as "power law" where K and n are empirical parameters, to fit the controlled release of drugs from various matrices up to 100%. (Abdullayev et al., 2009; Aguzzi et al., 2013; Li et al., 2016; Lvov et al., 2013; Peppas, 1985; Tan et al., 2014; Viseras et al., 2008; Wei et al., 2014) The R^2 of the fiting obtained using Peppas model to fit release data up to 60% was lower than that obtained with first order model (R^2= 0.9794) thus confirming that the model following the approach proposed in Aguzzi et al., 2013 allowed a good fitting of the experimental data and a physicochemical explanation of the SA release process from Hal lumen.

3.2 Hal/SA antibacterial activity

The results obtained by IMC measurements on the effect of SA on the metabolic behaviour of P. *fluorescens* IMA 19/5 are reported in this section.

The heat flow curves and the curves of the cumulative heat produced over time by the metabolic activity of *P. fluorescens* IMA 19/5 in TSB with and without the addition of pristine Hal are compared in Figure 3. The total heat produced, Q_{max}, can be related to the number of cells produced and the cumulative heat curves (figure 3B and figure S1 in Electronic Supplementary Information, ESI) are analogues to the conventional growth curves of the increase of bacterial number over time (Braissant et al., 2010; Gardikis et al., 2017; Von Ah et al., 2009). The mean slopes (Q/t) of the different portions of the cumulative heat curve represent the rates of heat production and are indicative of the bacterial growth rates.

The metabolic profile of *P. fluorescens* IMA 19/5 in TSB showed four phases (Figure 3A): an exponential growth phase in the time range 0-17000 s (with a maximum power reached, P_{max}, of 130 uW), a stationary phase from 20000 to 50000 s, a second growth phase from 50000 to 60000 s (up to P_{max}=230 uW) and a decline phase from 60000 to 70000 s.

When Hal was added, the metabolic profile of *P. fluorescens* IMA 19/5 changed importantly (figure 3A). The first growth phase was still centred at 10000 s but the rate of heat production was higher (P_{max}= 175 µW), the stationary phase was shortened, the second growth phase resulted anticipated at 30000 s with a P_{max}=270 µW) and the heat production stopped at lower time (50000 s instead of 70000 s). Nevertheless the cumulative heat produced, Qmax, remained the same, accounting for almost 9 J. (figure 3B).

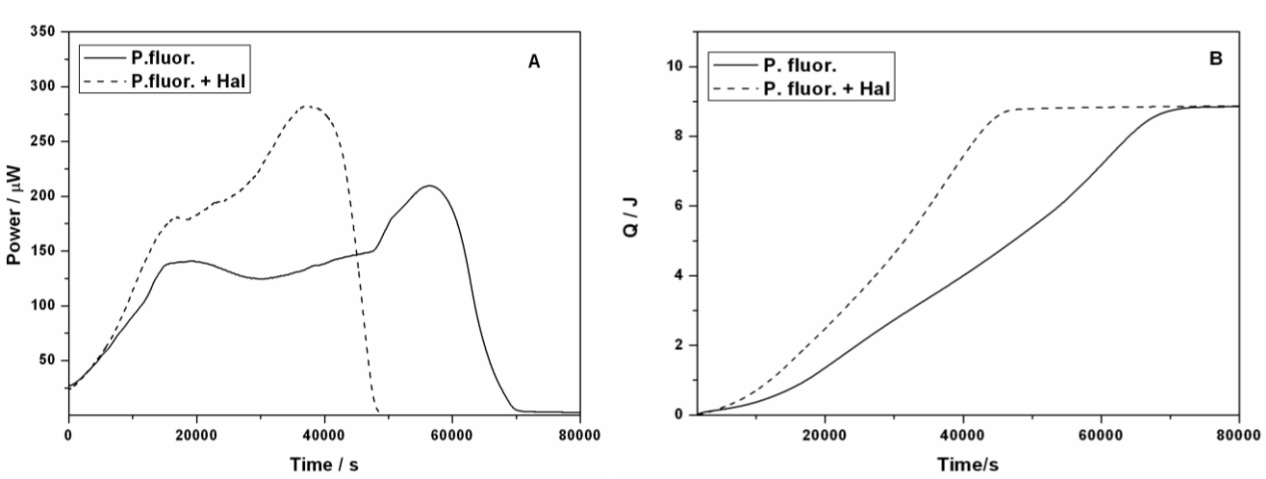

Figure 3: Heat flow curve (A) and cumulative heat produced curve over time (B) of the metabolic activity of *P. fluorescens* IMA 19/5 (continuous line) in TSB and in TSB added with pristine Hal (dashed line).

The features of the heat curve *P. fluorescens* IMA 19/5 in TSB added with pristine Hal seemed to confirm the bioinformatic analysis performed by Lai and coworkers (Lai et al., 2013), showing that halloysite stimulated processes related to cell growth and proliferation, representing one of the characteristics of an overall adaptive response to exposure.

The metabolic profile of *P. fluorescens* IMA 19/5 changed again when NaSA was inoculated both free and loaded inside Hal (Figure 4 and figure S1 in ESI).

Up to a concentration of 20 mM of free NaSA and of 10 mM of SA loaded into Hal, the first growth phase resulted faster and prolonged up to 20000 s with P_{max} in the range 250-300 µW. The first growth phase was followed by a decline phase, then the second growth phase started between 20000 and 40000 s. The stop of the heat production was anticipated below 65000 s depending on the NaSA concentration and on its availability. The effect of the presence of NaSA on all the metabolic steps was enhanced when NaSA was released by Hal.

At higher SA concentrations (30 mM for free NaSA, or 20 mM for SA loaded into Hal), a single exponential growth metabolic phase, starting after 30000 s, was present followed by an exponential decay (Figure 4 C, D). Above these concentrations a very low heat flow (or no heat flow) was registered (e.g. Figure 4D for Hal/SA 30 mM).

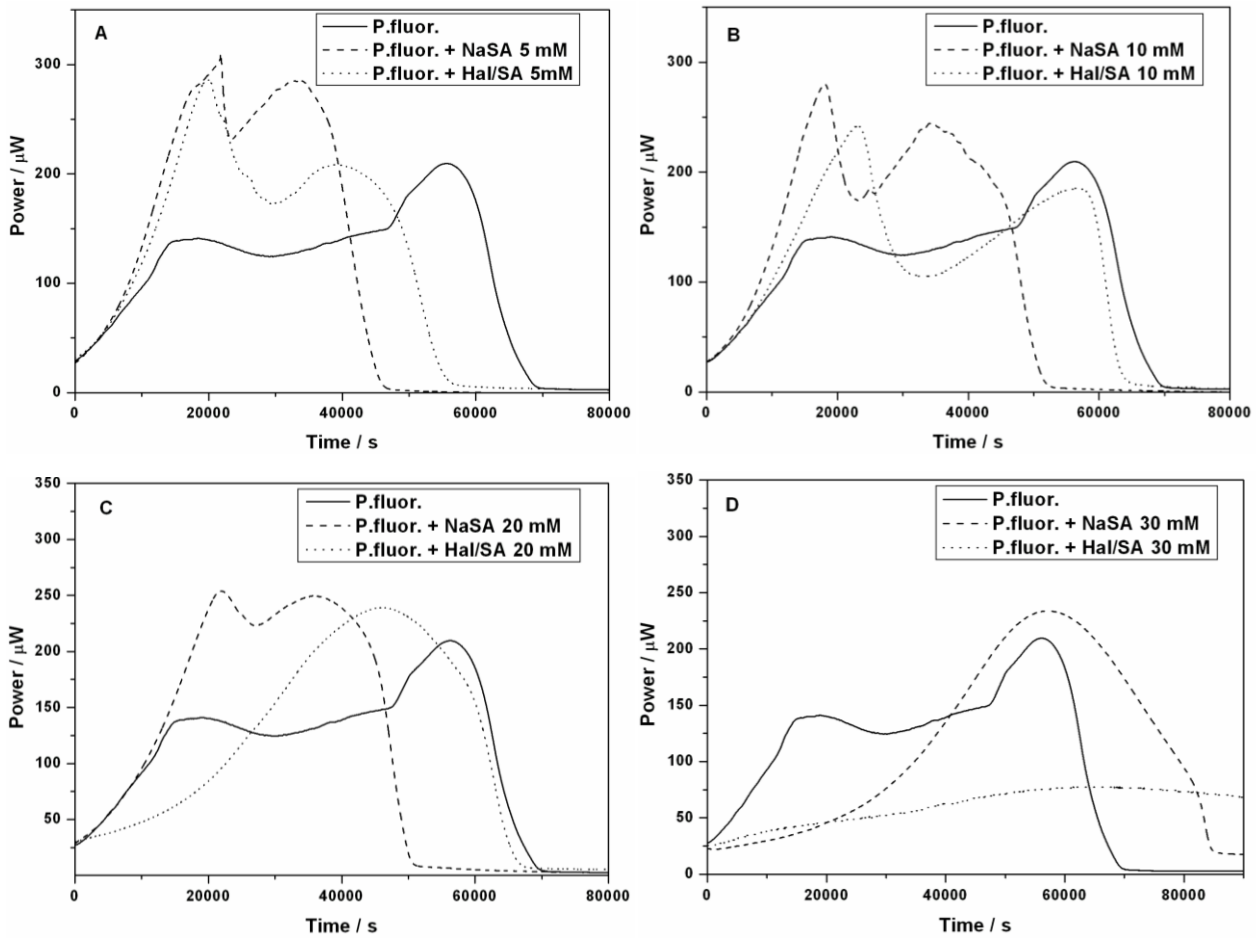

Figure 4: Heat flow curve of the metabolic activity of *P. fluorescens* IMA 19/5 in TSB compared to those of *P. fluorescens* IMA 19/5 in TSB added with: A), SA 5 mM,an aliquot of Hal/SA to give a final salycilate concentration of 5 mM; B) SA 10 mM, an aliquot of Hal/SA to give a final salycilate concentration of 10 mM; C) SA 20 mM, an aliquot of Hal/SA to give a final salycilate concentration of 20 mM; D) 30 mM, an aliquot of Hal/SA to give a final salycilate concentration of 30 mM.

These results suggested that at low concentrations (5 and 10 mM) SA, both free and loaded inside Hal, "enhanced" the metabolic activities of *P. fluorescens* IMA 19/5, by accelerating and prolonging over time the growth phases. Such an effect was more evident with free SA than when SA was released by Hal. Moreover, when SA concentration ranged from 5 to 10 mM the heat flow curves showed two picks, as for a diauxic event (Braissant et al., 2013), suggesting a possible utilization of SA by *P. fluorescens* IMA 19/5. On the other hand, the ability of strains belonging to *Pseudomonas* spp, to degrade SA was already reported by other authors (Filonov et al., 2000; Kesseru et al., 2005). Differently, when SA was added at higher concentrations (in the range 20 - 30 mM for SA loaded inside Hal and more than 30 mM for free SA), *P. fluorescens* IMA 19/5 metabolic activity was strongly inhibited (no heat produced by the bacteria), as shown by the flattening of the relative heat

flow curves. A tentative explanation of the enhanced antibacterial activity of Hal/SA with respect to free SA could be found in the heterogeneity of the system.

Under static conditions, Hal/SA system tends to migrate to the bottom of the reaction vessel, thus creating a gradient of SA concentration from the bottom to the top of the vessel. Under static conditions, the bacteria also lie at the bottom of the reaction vessel, on the surface of Hal very close to the release site, and perceive a local SA concentration that is unknown and likely much more high than the nominal one. By contrast, when SA is in solution, the bacteria perceive the same concentration in all the parts of the reaction vessel.

4. Conclusions

In this work the properties of Hal/SA system in aqueous solution and its antibacterial activity against *P. fluorescens* IMA 19/5 were investigated. The Hal/SA system was able:

- to stabilize Hal suspension in water;
- to release SA over 50 h with the typical behavior of molecules loaded into Hal. The SA release profile was well described by a simple model proposed by Viseras group which accounted for three sequential first order desorption processes: a first release from the external particle surface, followed by the release from tube fines, and finally by a slower release from the interior of Hal lumen;
- to show antibacterial activity at lower concentration than free SA.

Hal/SA system seems to be a promising system for the controlled release of SA in active packaging. In particular, water-soluble antimicrobials (as SA) have been indicated as the most appropriate when direct contact with food is involved (as in the case of meat). Indeed, when the additive is added to a polymeric formulation to be successively released into the food, it migrates only in the contact area between the food and the packaging material. Moreover, SA remains inside Hal's lumen until the system is anhydrous, and is released only when the Hal/SA system comes into contact with aqueous substrates. In such a system, the antibacterial activity is enhanced compared with free SA and obtained using lower SA concentrations.

AKNOWLEDGEMENTS

This work was supported by the project FIRB 2012 (No. RBFR12ETL5), funded by the Italian Ministry of University and Research.

REFERENCES

Abdullayev, E., Lvov, Y., 2016. Halloysite for Controllable Loading and Release. In: Yuan, P., Thill, A. (Eds) Nanosized Tubular Clay Minerals. Halloysite and Imogolite, Developments in clay science series Elsevier, 554-605 (Chapter22)

Abdullayev, E., Lvov, Y., 2011. Halloysite clay nanotubes for controlled release of protective agents. J. Nanosci. Nanotechnol. 11, 10007-10026.

Abdullayev, E.; Joshi, A.; Wei, W., Zhao, Y., Lvov, Y., 2012. Enlargement of halloysite clay nanotube lumen by selective etching of aluminum oxide. ACS Nano 6, 7216−7226.

Abdullayev, E., Price, R., Shchukin, D., Lvov, Y., 2009. Halloysite Tubes as Nanocontainers for Anticorrosion Coating with Benzotriazole. ACS Appl. Mater. Interfaces. 1(7), 1437-1443.

Aguzzi, C., Viseras, C., Cerezo, P., Valenzuela, C., 2013. Release kinetics of 5-aminosalicylic acid from halloysite. Colloids Surf. B Biointerface. 105, 75-80.

Baxter, G. J., Graham, A. B., Laerence, J. R., Wile,s D., Paterson, J. R., 2001. Salicylic acid in soups prepared from organically and non-organically grown vegetables. Eur. J. Nutr. 40, 289-292.

Biber, M. V., Stumm, W. 1994. An in-situ ATR-FTIR study: the surface coordination on aluminum and iron (III) oxides. Environ. Sci. Technol. 28, 763-768.

Biddeci, G., Cavallaro, G., Di Blasi, F., Lazzara, G., Massaro, M., Milioto, S., Parisi, F., Riela, S., Spinelli, G., 2016. Halloysite nanotubes loaded with peppermint essential oil as filler for functional biopolymer film. Carbohyd. Polym. 152, 548-557.

Braissant, O., Wirz, D., Gopfert, B., Daniels,, A.U. 2010a. Use of isothermal microcalorimetry to monitor microbial activities. FEMS Microbiol. Lett. 303, 1-8.

Braissant, O., Wirz, D., Gopfert, B., Daniels, A.U., 2010b. Biomedical Use of Isothermal Microcalorimeters. Sensor. 10, 9369-9383. doi:10.3390/s101009369

Braissant, O., Bonkat, G., Wirz, D., Bachmann, A., 2013. Microbial growth and isothermal microcalorimetry: Growth models and their application to microcalorimetric data. Thermochim. Acta 555, 64–71.

Bretti, C., Cataldo, S., Gianguzza, A., Lando, G., Lazzara, G. Pettignano, A. Sammartano, S., 2016. Thermodynamics of Proton Binding of Halloysite Nanotubes. J. Phys. Chem. C. 120, 7849-7859.

Cavallaro, G., Lazzara, G., Milioto, S. 2012. Exploiting the colloidal stability and solubilization ability of clay nanotubes/ionic surfactant hybrid nanomaterials. J. Phys. Chem. C. 116, 21932-21938.

Coleman, W. P. 3rd, Brody, H.J., 1997. Advances in chemical Peeling. Dermatol. Clin. 15, 19-26.

De Azeredo, H. M. C., 2009. Nanocomposites for food packaging application. Food Research International, 42, 1240-1253.

Della Porta, V., Bramanti, E., Campanella, B., Tiné, M.R., Duce, C., 2016. Conformational analysis of bovine serum albumin adsorbed on halloysite nanotubes and kaolinite: a Fourier transform infrared spectroscopy study. RSC Adv. 6, 72386-72398

Duce, C., Vecchio Ciprioti, S., Ghezzi, L., Ierard,i V., Tinè, M.R., 2015. Thermal behavior study of pristine and modified halloysite nanotubes. A modern kinetic study. J. Therm. Anal. Calorim. 121, 1011-1019. DOI 10.1007/s10973-015-4741-7

Duce, C., Della Porta, V., Bramanti, E., Campanella, B., Spepi, A., Tiné, M.R., 2017. Loading of Halloysite Nanotubes with BSA, α-Lac and β-Lg: a Fourier Transform Infrared Spectroscopic and thermogravimetric study. Nanotech. 28, 055706-055718. doi:10.1088/1361-6528/28/5/055706

Ernst, Z.L., Menashi, J., 1963. Spectrophotometric determination of the dissociation constants of some substituted salicylic acids. Part 2. Trans. Faraday Soc. 59, 230-240.

Filonov, A.E., Karpov, A., Kosheleva, I.A., Boronin, A.M., 2000. The efficiency of salicylate utilization by Pseudomonas putida strains catabolizing naphthalene via different biochemical pathways process. Biochem. 35, 983–987. doi: 10.1016/S0032-9592(00)00130-8

Galotto, M. J., Guarda, A.; Lopez de Dicastillo, C., 2015. Antimicrobial Active Polymers in Food Packaging. In Cirillo, G.; Spizzirri, U. G., Iemma, F. (Eds) Functional Polymers in Food Science: From Technology to Biology (Set), Wiley, 323-353. (Chapter10)

Gardikis, K., Signorelli, M., Ferrario, C., Schiraldi, A., Forina, M.G., Hatziantoniu, S., Demetzos, C., Fessas, D. 2017. Microbial biosensors to monitor the encapsulation effectiveness of Doxorubicin in chimeric advanced Drug Delivery Nano Systems: A calorimetric approach. Int. J. Pharm. 516, 178-184.

Gram, L., Ravn, L., Rasch, M., Bruhn, J.B., Christensen, A.B., Givskov, M., 2002. Food spoilage-interactions between food spoilage bacteria. Int. J. Food Microbiol. 78, 79- 97.

Kesseru, P., Kiss, I., Bihari, Z., Pàl, K., Portoro, P., Polyàk, B., 2005. Nitrate-dependent salicylate degradation by Pseudomonas butanovora under anaerobic conditions. Bioresour. Technol. 96, 779–784. https://doi.org/10.1016/j.biortech.2004.08.009

Kubicki, J. D., Itoh, M. J., Schroeter, L. M., Apitz, S. E. 1997. Bonding mechanism of salycilic acid adsorbed onto illite clay: an ATR-FTIR and molecular orbital study. Environ. Sci. Technol. 31, 1151-1156.

Lai, X., Agarwal, M., Lvov, Y. M., Pachpande, C., Varahramyan, K., Witzmann, F. A., 2013. Proteomic profiling of halloysite clay nanotube exposure in intestinal cell co-culture. J. Appl. Toxicol. 33, 1316 –1329. doi:10.1002/jat.2858

Li, X., Ouyang, J., Yang, H., Chnag, S., 2016. Chitosan modified halloysite nanotubes as emerging porous microspheres for drug carrier. Appl. Clay Sci. 126, 306-312.

Lun, H., Ouyang, J., Yang, H., 2014. Natural halloysite nanotubes modified as an aspirin carrier. RSC Adv. 4, 44197- 44202. doi:10.1039/C4RA09006C

Lvov, Y., Abdullayev, E., 2013. Functional polymer-clay nanotube composites with sustained release of chemical agents. Prog. Polym. Sci. 38, 1690-1719.

Lvov, Y., Aerov, A., Fakhrullin, A., 2014. Clay nanotube encapsulation for functional biocomposites. Adv. Colloid Interface Sci. 207, 189-198

Lvov, Y. M., DeVilliers, M. M., Fakhrullin, R., 2016, The application of halloysite tubule nanoclay in drug delivery. Expert Opin. Drug Delivery, 13, 977.

Makaremi, M., Pasbakhsh, P., Cavallaro, G., Lazzara, G., Kit Aw, Y., Mae S.L., Milioto, S., 2017. ACS Appl. Mater. Interfaces. 9 (20), 17476-17488. doi: 10.1021/acsami.7b04297

Massaro, M., Lazzara, G., Milioto, S., Noto, R., Riela, S., 2017. Covalently modified halloysite clay nanotubes: synthesis, properties, biological and medical applications. J. Mat. Chem. B. 5, 2867-2882. doi.10.1039/C7TB90071F

Meister Meira, S. M., Zehetmeyer, G., Orlandini Werner, J.,Brandelli, A., 2017. A novel active packaging material based on starch-halloysite nanocomposites incorporating antimicrobial peptides. Food Hydrocolloids, 63, 561-570

Pasbakhsh, P., De Silva, R., Vahedi, V., Jock Churchman G., 2016. Halloysite nanotubes: prospects and challenges of their use as additives and carriers–A focused review. Clay Minerals 51 (3), 479-487

Peppas, N.A. 1985. Analysis of Fickian and non-Fickian drug release from polymers. Pharm. Acta Helv. 60, 110-111.

Presti, A., Pedone,, A., Mancini G., Duce,, C., Tiné M.R., Barone, V., 2016. Insights on structural and dynamical features of water at halloysite interfaces probed by DFT and classical Molecular Dynamics simulations. Phys. Chem. Chem. Phys.18, 2164-2174.

Riela, S., Massaro, M., Colletti, C.G., Bommarito, A., Giordano, C., Milioto, S., Noto, R., Poma, P., Lazzara, G., 2014. Development and characterization of co-loaded curcumin/triazolehalloysite systems and evaluation of their potential anticancer activity. Int. J. Pharm. 475, 613-623. https://doi.org/10.1016/j.ijpharm.2014.09.019

Rong, X.M., Huang, Q.Y., Jiang, D.H., Cai, P., Liang, W., 2007. Isothermal microcalorimetry: a review of applications in soil and environmental sciences. Pedosphere 17, 137–145.

Spepi, A., Duce, C., Pedone, A., Presti, D., Gonzalez-Rivera, J., Ierardi, V., Tiné, M.R., 2016. Experimental and DFT Characterization of Halloysite Nanotubes Loaded with Salicylic Acid. J. Phys. Chem. C. 120, 26759−26769.

Tan, D., Yuan, P., Annabi-Bergaya, F., He, H., 2014. Loading and in vitro release of ibuprofen in tubular halloysite. Appl. Clay Sci. 96, 50-55 doi: 10.1016/j.clay.2014.01.018

Vazquez, C., Lago, N., Mato, M.M., Casas, L.M., Esarte, L., Legido, J.L., Arias, I., 2014. Microcalorimetric performance of growth in culture of Escherichia coli, Proteus mirabilis and their mixtures in different proportions. J. Therm. Anal. Calorim. 116, 107-112.

Vergaro, V., Abdullayev, E., Lvov, Y., Zeitoun, A., Cingolani, R., Rinaldi, R., Leporatti, S., 2010. Cytocompatibility and uptake of halloysite clay nanotubes. Biomacromolecules. 11, 820-826. doi: 10.1021/bm9014446

Viseras, M.T., Aguzzi, C., Cerezo, P., Valenzuela, C., 2008. Equilibrium and kinetics of 5-aminosalicylic acid adsorption by halloysite. Microporous and Mesoporous Mater. 108, 112-116

Von Ah U., Wirz D., Daniels A.U. 2009. Isothermal micro calorimetry – a new method for MIC determinations: results for 12 antibiotics and reference strains of E. coli and S. aureus. BMC Microbiol. 9, 106. doi: 10.1186/1471-2180-9-106.

Wei, W., Minullina, R., Abdullayev, E., Fakhrullin, R., Mills, D., Lvov, Y., 2014. Enhanced efficiency of antiseptics with sustained release from clay nanotubes. RSC Adv. 4, 488 – 494. doi: 10.1039/C3RA45011B

Yost, E. C., Tejedor-Tejedor,, M. I., Anderson M. A., 1990. In situ CIR-FTIR characterization of salycilate complexes at the goethite/aqueous solution interface. Environ. Sci. Technol. 24, 822-828.

Yuan, P., Tan, D., Annabi-Bergaya, F., 2015. Properties and applications of halloysite nanotubes: recent research advances and future prospects." Applied Clay Science 112-113, 75-93.

Yuan, P., Southon, P. D., Liu, Z., Kepert, C. J., 2012. Organosilane functionalization of halloysite nanotubes for enhanced loading and controlled release. Nanotechnology 37, 375705.

Zhang, Y., Tang, A., Yang, H., Ouyang, J., 2016. Applications and interfaces of halloysite nanocomposites. Appl. Clay Sci. 119, 8-17. https://doi.org/10.1016/j.clay.2015.06.034